Chapter 4

Helicity Analysis

Since the $\rho\rho$ final state is a vector-vector system, thus, the two ρ mesons can be in a mixture of S, P, and/or D waves. Both longitudinal and transverse polarizations of the ρ meson are possible. In the B rest frame, if we take the ρ^+ flight direction as z-axis (Fig.4.1), due to angular momentum conservation, the possible z components of the angular momenta of the ρ^0 and ρ^+ are, for the longitudinal polarization state

$$J_z(\rho^0) = 0, \quad J_z(\rho^+) = 0,$$

and for the transverse polarization states,

$$J_z(\rho^0) = 1, \quad J_z(\rho^+) = -1,$$

$$J_z(\rho^0) = -1, \quad J_z(\rho^+) = 1.$$

From the momentum conservation, we know the ρ^0 and ρ^+ fly in opposite directions, thus the helicity (H) is

$$H(\rho^0) = 0, \quad H(\rho^+) = 0,$$

$$H(\rho^0) = 1, \quad H(\rho^+) = 1,$$

$$H(\rho^0) = -1, \quad H(\rho^+) = -1.$$

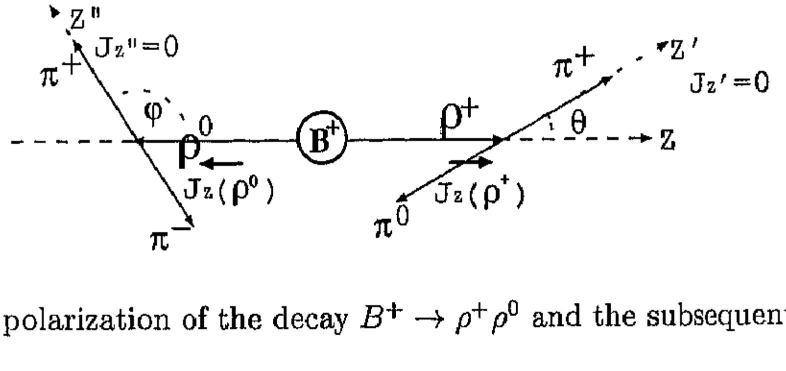

Figure 4.1: The polarization of the decay $B^+ \to \rho^+\rho^0$ and the subsequent decay $\rho \to \pi\pi$.

Subsequently, the two vector ρ mesons decay to two pseudo-scalar π mesons. Below, we discuss the helicity angle in the decay $\rho^+ \to \pi^+\pi^0$ in the ρ^+ rest frame.

The process is from an initial state with $|J(\rho^+) = 1, J_z(\rho^+)\rangle$ to a final state with $|J(\pi^+\pi^-) = 0, J_{z'}(\pi^+\pi^-) = 0\rangle$ (Fig. 4.1), where the z, z' axes are along the ρ^+ and outgoing π^+, $J(\pi^+\pi^-)$ and $J_{z'}(\pi^+\pi^-)$ are the net angular momentum and its z-component. The amplitude for ρ^+ decaying at angle θ is given by the d function $(d^{J(\rho^+)}_{J'_z(\pi^+\pi^-),J_z(\rho^+)})$. For the three possible ρ helicity $J_z(\rho^+) = -1, 0, 1$,

$$d^1_{0,-1} = -\frac{\sin\theta}{\sqrt{2}}, \quad d^1_{0,0} = \cos\theta, \quad d^1_{0,1} = \frac{\sin\theta}{\sqrt{2}}.$$

Squaring the amplitudes, we obtain the helicity angle distributions,

$$\begin{aligned} H(\rho^+) = -1, &\quad \frac{\sin^2\theta}{2} \\ H(\rho^+) = 1, &\quad \frac{\sin^2\theta}{2} \\ H(\rho^+) = 0, &\quad \cos^2\theta \end{aligned}$$

Since the helicity angle follows the same distribution $\sin^2\theta/2$, for the two transverse polarization states $H(\rho) = -1, 1$, we make no distinction between $H = 1$ and $H = -1$, denote as H_{11}; and denote the longitudinal polarization state as H_{00}.

For the decay $\rho^0 \to \pi^+\pi^-$, the helicity angle distributions are the same: $\sin^2\theta/2$ for $H(\rho^0) = \pm 1$ and $\cos^2\theta$ for $H(\rho^0) = 0$. Experimentally, the helicity-angle is the angle between the directions of one of the decay pions in the ρ rest frame and the ρ meson in the B rest frame.

The H_{00} polarization state is expected to be dominant [45]. In the following, we perform a helicity-angle analysis to isolate the helicity states.

4.1 Fits to Helicity-angle

The helicity analysis is performed by looking at the $\rho \to \pi\pi$ helicity-angle distributions. For the H_{00} helicity state, each ρ decay direction tends to align with its momentum direction; for the H_{11} helicity state, the ρ decay direction tends to be perpendicular to its flight direction. The ρ^0 and ρ^+ cosine helicity-angle distributions from signal-MC are shown in Fig. 4.2, where the data points represent the yields from the ΔE fit with a shape determined from H_{00} signal-MC sample. The absence of events near $\cos\theta_{hel(\rho^+)} = 1$ is due to the π^0 momentum requirement.

Therefore, based on the ρ meson helicity-angle information, we can measure the decay amplitude for each helicity state.

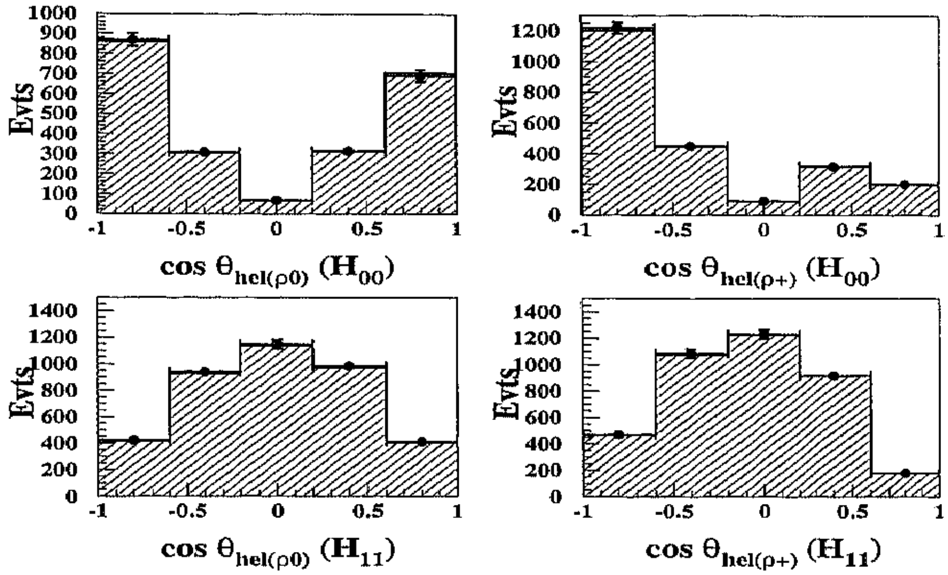

Figure 4.2: The cosine ρ^0 (left) and ρ^+ (right) helicity-angle distributions. The data points show the yields of ΔE fits applied to different helicity bins of signal MC with a shape determined from H_{00} signal-MC.

In addition, the ΔE resolution depends on π^0 momentum, increasing from $\sigma = 16\,\text{MeV}$ to $\sigma = 32\,\text{MeV}$, while the π^0 momentum varies from $0.5\,\text{GeV/c}$ to $2.8\,\text{GeV/c}$, as shown in Fig. 4.3. Thus, in determining the signal yields for different ρ^+ cosine helicity-angle bins, a bin-by-bin MC-determined ΔE width is used.

Figure 4.4 shows the two background-subtracted ρ cosine helicity-angle distributions for selected events in the $5.272\,\text{GeV/c}^2 < M_{bc} < 5.290\,\text{GeV/c}^2$ signal region. A simultaneous χ^2 fit is performed using MC-determined expectations for the H_{00} and H_{11} helicity states. The solid histograms show the fit results, indicate that the H_{00} state dominates.

4.2 Statistical Errors

The signal yields from the fits to the ρ helicity-angle distributions are

$$N_{00} = 48.29 \pm 10.78,$$

$$N_{11} = 4.31 \pm 8.71.$$

The ratios are

$$r_{00} = \frac{N_{00}}{N_{00} + N_{11}}; \quad r_{11} = \frac{N_{11}}{N_{00} + N_{11}},$$

where N_{00} (N_{11}) is the number of the signal yield for the H_{00} (H_{11}) helicity state.

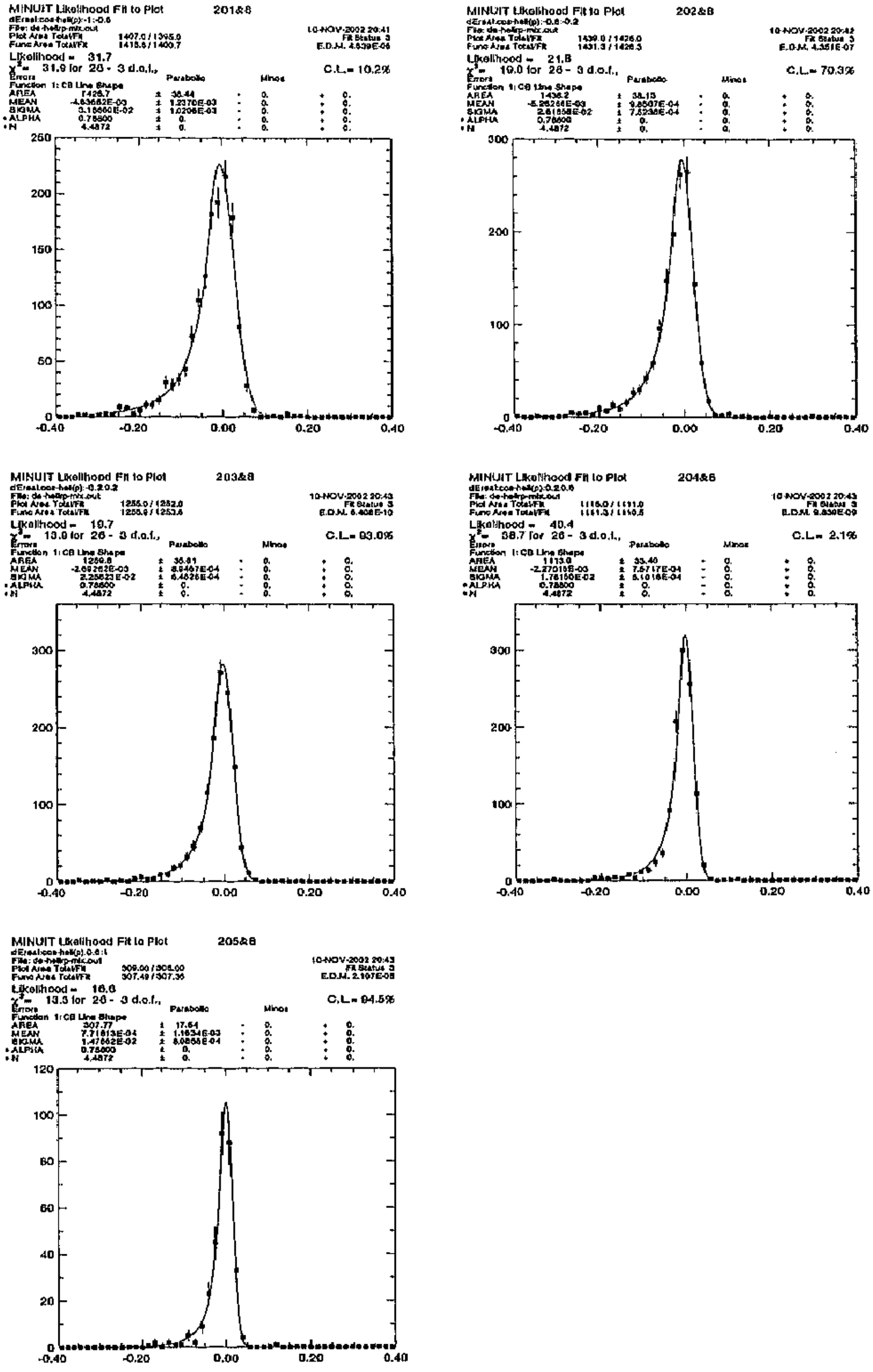

Figure 4.3: The ΔE resolution varies over the ρ^+ helicity-angle. The plots from top to bottom are for $-1.0 < \cos\theta_{hel(\rho^+)} < -0.6$; $-0.6 < \cos\theta_{hel(\rho^+)} < -0.2$; $-0.2 < \cos\theta_{hel(\rho^+)} < 0.2$; $0.2 < \cos\theta_{hel(\rho^+)} < 0.6$; $0.6 < \cos\theta_{hel(\rho^+)} < 1.0$.

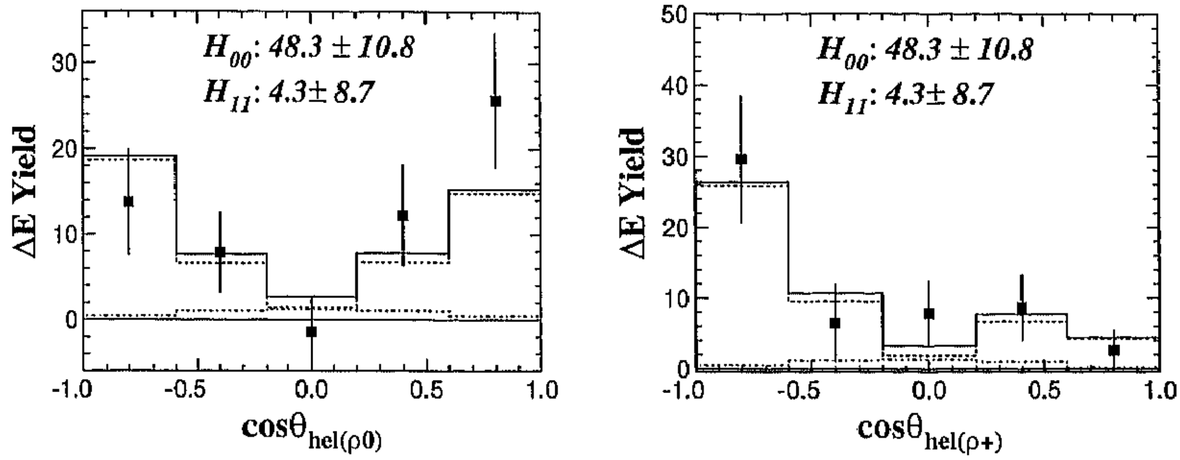

Figure 4.4: The data points show the background-subtracted cosine helicity-angle distributions for ρ^0 (left) and ρ^+ (right). In each plot, the upper (lower) dashed histogram is the H_{00} (H_{11}) component of the fit; the solid histogram is their sum. The absence of events near $\cos\theta_{hel(\rho^+)} = 1$ is due to the π^0 momentum requirement.

The errors are propagated as

$$(\Delta r_{00})^2 = (\frac{\partial r_{00}}{\partial N_{00}})^2(\Delta N_{00})^2 + (\frac{\partial r_{00}}{\partial N_{11}})^2(\Delta N_{11})^2 + 2\,\mathrm{cov}(N_{00}, N_{11})\frac{\partial r_{00}}{\partial N_{00}}\frac{\partial r_{00}}{\partial N_{11}},$$

$$(\Delta r_{11})^2 = (\frac{\partial r_{11}}{\partial N_{00}})^2(\Delta N_{00})^2 + (\frac{\partial r_{11}}{\partial N_{11}})^2(\Delta N_{11})^2 + 2\,\mathrm{cov}(N_{00}, N_{11})\frac{\partial r_{11}}{\partial N_{00}}\frac{\partial r_{11}}{\partial N_{11}}.$$

By solving these, we obtain

$$\Delta r_{00} = \frac{1}{(N_{00}+N_{11})^2}\sqrt{(N_{11}\Delta N_{00})^2 + (N_{00}\Delta N_{11})^2 - 2\,N_{00}N_{11}\mathrm{cov}(\mathrm{N_{00}}, \mathrm{N_{11}})},$$

$$\Delta r_{11} = \Delta r_{00}.$$

Note that the covariance $\mathrm{cov}(N_{00}, N_{11})$ is non-zero, $\mathrm{cov}(N_{00}, N_{11}) = -56.0$.

By inserting the numbers, we obtain

$$r_{00} = (91.8 \pm 16.3(\mathrm{stat.}))\%,$$

$$r_{11} = (8.2 \pm 16.3(\mathrm{stat.}))\%.$$

These r_{00} and r_{11} are not the true polarization ratios, since they are diluted by the different efficiencies for the H_{00} and H_{11} states. As discussed in the preceding section, the efficiency of the H_{11} helicity state is 1.9 times that of the H_{00} state. By taking the efficiencies into account, the polarization ratios can be expressed as

$$\frac{\Gamma_L}{\Gamma} = \frac{N_{00}\epsilon_{11}}{N_{00}\epsilon_{11} + N_{11}\epsilon_{00}}\ ;\ \frac{\Gamma_T}{\Gamma} = \frac{N_{11}\epsilon_{00}}{N_{00}\epsilon_{11} + N_{11}\epsilon_{00}}, \tag{4.1}$$

where ϵ_{00} (ϵ_{11}) is the efficiency for the H_{00} (H_{11}) helicity state.

The statistical errors can be derived as

$$\Delta(\frac{\Gamma_L}{\Gamma}) = \frac{\epsilon_{00}\epsilon_{11}}{(N_{00}\epsilon_{11}+N_{11}\epsilon_{00})^2}\sqrt{(N_{11}\Delta N_{00})^2+(N_{00}\Delta N_{11})^2-2\,\mathrm{cov}(\mathrm{N}_{00},\mathrm{N}_{11})N_{00}N_{11}},$$

$$\Delta(\frac{\Gamma_T}{\Gamma}) = \Delta(\frac{\Gamma_L}{\Gamma}).$$

Thus, we obtain

$$\frac{\Gamma_L}{\Gamma} = (94.8 \pm 10.6(\text{stat.}))\%,$$

$$\frac{\Gamma_T}{\Gamma} = (5.2 \pm 10.6(\text{stat.}))\%.$$

The results are summarized in Table 4.1.

	H_{00}	H_{11}
Signal yields	48.29 ± 10.78	4.31 ± 8.71
Obs. ratio (no correct)	$(91.8 \pm 16.3)\%$	$(8.2 \pm 16.3)\%$
Pol. ratio (effic correct)	$(94.8 \pm 10.6)\%$	$(5.2 \pm 10.6)\%$

Table 4.1: The results of the polarization ratio.

4.3 Systematic Errors

The systematic errors for helicity analysis are caused by signal extraction, and efficiency errors.

As mentioned, the helicity analysis is based on the signal yields from the ΔE fit with a shape determined from the H_{00} signal-MC. The systematic error due to signal extraction is estimated by extracting signal yields with a $H_{00} + H_{11}$ (1:1) MC determined ΔE shape and measuring the difference in polarization ratio. The results are listed in Table 4.2. We quote the difference of 2.1% as the systematic error.

	H_{00}	H_{11}
Signal yields	45.88 ± 10.10	2.39 ± 7.98
Obs. ratio (no correct)	$(95.1 \pm 16.4)\%$	$(4.9 \pm 16.4)\%$
Pol. ratio (effic correct)	$(96.9 \pm 10.4)\%$	$(3.1 \pm 10.4)\%$

Table 4.2: Cross-check results of the polarization ratios by using a $(H_{00}+H_{11})$-determined ΔE shape, which is used to estimate the systematic errors on the signal extraction.

We discussed that the efficiency error includes uncertainties in the efficiencies of the signal-MC sample statistics, continuum rejection, particle identification, tracking and π^0 detection. For the polarization ratio, since the uncertainty in continuum rejection efficiency, particle identification efficiency, tracking efficiency and π^0 detection efficiency are mostly canceled, we only consider the signal MC statistical error. These contributions to the systematic error are

$$\Delta(\frac{\Gamma_L}{\Gamma}) = \frac{N_{00}N_{11}}{(N_{00}\epsilon_{11} + N_{11}\epsilon_{00})^2}\sqrt{(\epsilon_{11}\Delta\epsilon_{00})^2 + (\epsilon_{00}\Delta\epsilon_{11})^2},$$

and

$$\Delta(\frac{\Gamma_T}{\Gamma}) = \Delta(\frac{\Gamma_L}{\Gamma})$$

The systematic error caused by the efficiency uncertainty is found to be less than 0.2%. The total systematic errors are listed in Table 4.3.

	Relative (to $\frac{\Gamma_L}{\Gamma}$) Errors
ΔE shape	2.2%
ϵ error	0.2%
Total	2.2%

Table 4.3: The systematic errors in polarization ratio

We obtain the polarization ratios of the decay $B^+ \to \rho^+\rho^0$,

$$\frac{\Gamma_\mathbf{L}}{\Gamma} = (\mathbf{94.8 \pm 10.6(stat.) \pm 2.1(sys.)})\%,$$

$$\frac{\Gamma_\mathbf{T}}{\Gamma} = (\mathbf{5.2 \pm 10.6(stat.) \pm 2.1(sys.)})\%.$$

4.4 Branching Fraction Results

We calculate the branching fraction by

$$\begin{aligned}
\mathcal{B} &= \frac{N^{yield}}{N_{BB}} \frac{1}{(\Gamma_L/\Gamma)\epsilon_{00} + (\Gamma_T/\Gamma)\epsilon_{11}} \\
&= \frac{N^{yield}}{N_{BB}} \frac{1}{\frac{N_{00}/\epsilon_{00}}{N_{00}/\epsilon_{00} + N_{11}/\epsilon_{11}}\epsilon_{00} + \frac{N_{11}/\epsilon_{11}}{N_{00}/\epsilon_{00} + N_{11}/\epsilon_{11}}\epsilon_{11}} \\
&= \frac{N^{yield}}{N_{BB}} \frac{N_{00}/\epsilon_{00} + N_{11}/\epsilon_{11}}{N_{00} + N_{11}} \\
&= \frac{N^{yield}}{N_{BB}}(\frac{r_{00}}{\epsilon_{00}} + \frac{r_{11}}{\epsilon_{11}}),
\end{aligned}$$

where N^{yield} is the signal yield from the ΔE fit, N_{BB} is the number of $B\bar{B}$, ϵ_{00} (ϵ_{11}) is the efficiency for the H_{00} (H_{11}) helicity state, and r_{00} (r_{11}) is the observed ratio of the H_{00} (H_{11}) helicity state.

Contributions to the systematic error are caused by uncertainties in the efficiencies of signal-MC statistics, PID, continuum rejection, tracking, π^0 detection, ΔE fit, and the mixture of helicity states. We assign 3.6% systematic error for particle identification and signal-MC statistical error; 5.4% for the continuum rejection, estimated from the study of $B^+ \to \bar{D}^0\pi^+$, $\bar{D}^0 \to K^+\pi^-\pi^0$, by comparing the signal yields before and after continuum rejection is applied for MC and data; a 2%/track for the tracking systematic error [46]; a 4.0% systematic error to account for π^0 reconstruction [47]; $^{+7.3}_{-6.7}\%$ for the ΔE fit systematic error, obtained by varying each parameter of the fitting functions by $\pm 1\sigma$ and measuring the change in the signal yield, as listed in Table 4.4; and 1% systematic error for $N_{B\bar{B}}$.

Moreover, the error due to rare decay backgrounds is estimated by fitting the ΔE distribution with an additional component with the yield fixed to its MC-expectation. The change in signal yield is taken as systematic error to account for this contamination.

The branching fraction errors propagated from uncertainty in the efficiencies as

$$(\Delta\mathcal{B})^2 = (\frac{\partial\mathcal{B}}{\partial\epsilon_{00}}\Delta\epsilon_{00})^2 + (\frac{\partial\mathcal{B}}{\partial\epsilon_{11}}\Delta\epsilon_{11})^2,$$

thus,

$$\frac{\Delta\mathcal{B}}{\mathcal{B}} = \frac{\epsilon_{00}\epsilon_{11}}{r_{00}\epsilon_{11} + r_{11}\epsilon_{00}}\sqrt{(\frac{r_{00}}{\epsilon_{00}^2}\Delta\epsilon_{00})^2 + (\frac{r_{11}}{\epsilon_{11}^2}\Delta\epsilon_{11})^2}.$$

It is used to estimate the errors shown above.

The quadratic sum of these errors is taken as the total systematic error, as summarized in Table 4.5.

In addition, we estimate the branching fraction error due to the uncertain mixture of helicity states by shifting the ratio $\frac{\Gamma_L}{\Gamma}$ by 1σ or up to 100%, and assign the change in the branching fraction as the third error. Table 4.6 shows the results.

In summary, we obtain the branching fraction of $B^+ \to \rho^+\rho^0$,

$$\mathcal{B}(\mathbf{B}^+ \to \rho^+\rho^0) = (\mathbf{31.7 \pm 7.1(stat.) \pm 3.9(sys.)^{+1.0}_{-2.1}(pol.)) \times 10^{-6}}.$$

Parameter	Variation -1σ (%)	Variation $+1\sigma$(%)
signal:CB line+Gaussian		
mean	0.45	-0.52
sigma	-2.16	2.08
alpha	4.09	-3.49
N	4.15	-2.30
Gau/CB	-1.28	1.35
sigma1	-0.39	0.35
1st Chebyshev		
Cheb-1	-4.12	3.45
Smoothed histogram		
$B\bar{B}$ norm	-2.02	1.18
Total	+7.33; -6.72	

Table 4.4: The systematic error for the ΔE fit. This is obtained by varying the fixed parameters by $\pm 1\sigma$.

Source	Relative Systematic Error (%)
PID + MC-statistic	$\pm$ 3.6
Continuum rejection	$\pm$ 5.4
Tracking	$\pm$ 6.0
π^0 recon.	$\pm$ 4.0
ΔE fit	+7.3/-6.7
Rare decay bg.	-3.3
$N_{B\bar{B}}$	$\pm$ 1
Total	+12.2/ -12.3

Table 4.5: Summary of systematic errors

Polar. Γ_L/Γ	Branching Ratio	Difference in BR
$\Gamma_L/\Gamma - 1\sigma$	29.6×10^{-6}	-2.07×10^{-6}
$\Gamma_L/\Gamma = 1$	32.7×10^{-6}	1.04×10^{-6}

Table 4.6: The branching ratio error due to the uncertain mixture of helicity states, which is taken as a third error.